Proc. IRE (Corresp.), vol. 50, pp. 2523–2524, Dec. 1962.
[3] S. T. Eng and R. Solomon, "Frequency dependence of the equivalent series resistance for a germanium parametric amplifier diode," *Proc. IRE* (Corresp.), vol. 48, pp. 358–359, Mar. 1960.
[4] D. E. Sawyer, "Surface dependent losses in variable reactance diodes," *J. Appl. Phys.*, vol. 30, pp. 1689–1691, Nov. 1959.
[5] K. İnal and C. Toker, "Minimum noise figure of paramps with frequency dependent apparent R_s," *IEEE Trans. Microwave Theory Tech.* (Corresp.), vol. MTT-19, pp. 333–334, Mar. 1971.
[6] F. J. Hyde, S. Deval, and C. Toker, "Varactor diode measurements," *Radio Electron. Eng.*, vol. 31, pp. 67–75, Feb. 1966.
[7] R. I. Harrison, "Parametric diode Q measurements," *Microwave J.*, vol. 3, pp. 43–46, May 1960.
[8] R. Mavaddat, "Varactor diode Q-factor measurements," *J. Electron. Contr.*, vol. 15, pp. 51–54, July 1963.
[9] E. W. Sard, "A new procedure for calculating varactor Q from impedance versus bias measurements," *IEEE Trans. Microwave Theory Tech.*, vol. MTT-16, pp. 849–860, Oct. 1968.
[10] J. M. Roe, "Varactor Q measurement," *IEEE Trans. Microwave Theory Tech.* (Corresp.), vol. MTT-19, pp. 728–729, Aug. 1971.
[11] B. C. DeLoach, "A new microwave measurement technique to characterize diodes and an 800-Gc cutoff frequency varactor at zero volts bias," *IEEE Trans. Microwave Theory Tech.*, vol. MTT-12, pp. 15–20, Jan. 1964.
[12] C. Toker and F. J. Hyde, "The series resistance of varactor diodes," *Radio Electron. Engr.*, vol. 32, pp. 165–168, Sept. 1966.
[13] W. J. Getsinger, "The packaged and mounted diode as a microwave circuit," *IEEE Trans. Microwave Theory Tech.*, vol. MTT-14, pp. 58–69, Feb. 1966.
[14] H. N. Dawirs, "Equivalent circuit of a series gap in the center conductor of a coaxial transmission line," *IEEE Trans. Microwave Theory Tech.* (Corresp.), vol. MTT-17, pp. 127–129, Feb. 1969.
[15] T. Morena, *Microwave Transmission Design Data.* New York: Dover, 1958.
[16] E. L. Ginzton, *Microwave Measurements.* New York: McGraw-Hill, 1957, p. 279.
[17] D. G. Vice, "Parametric amplifier noise analysis," *IEEE Trans. Microwave Theory Tech.*, vol. MTT-13, pp. 162–167, Mar. 1965.
[18] L. H. Blackwell and K. L. Kotzebue, *Semiconductor Diode Parametric Amplifiers.* Englewood Cliffs, N. J.: Prentice-Hall, 1961.

A Moment Method with Mixed Basis Functions for Scatterings by Waveguide Junctions

Y. LEONARD CHOW AND SIEN-CHONG WU

***Abstract*—A moment method with mixed basis functions is introduced. In this formulation, modal basis functions are used for the expansion of the currents corresponding to the scattered propagating modes, while pulse basis functions are used for the expnsion of the current corresponding to the scattered envancescent waves. This, together with the Dirac δ weighting functions, reduces the number of total basis functions needed while retaining the simplicity and versatility of the method to cover junctions of an arbitrary shape. This method is applied to study examples of homogeneous and inhomogeneous waveguide junctions of parallel-plate waveguide propagating TE waves. It is found that for junctions that are not electrically large the convergence of the solutions is good.**

An appendix is included to transform and quicken the numerical integration of the modal basis functions.

I. Introduction

MOMENT METHODS have been used to study scattering problems for different types of scattering boundaries with accurate results. However, the basis functions used in each method have been limited to a single type. For instance, the unit-pulse basis functions have been used in the scattering by cylindrical obstacles in open space [1], [2]; the modal basis functions have been used in the scattering by two-dimensional (i.e., parallel-plate) waveguide diaphragms [3]–[5]. The former basis functions had to be used due to the "not-so-regular" shape of the cylindrical obstacle; the latter had to be used due to the infinite waveguide walls. From the above examples, it becomes evident that a mixed type of basis functions, consisting of both the unit pulses and the modes, would well be used for a cylindrical obstacle (along the third dimension) in a parallel-plate waveguide.

A first attempt in this direction for a single propagating TE_{10} mode was carried out by Wu and Chow [6]. In the present paper, the purpose is to extend and formulate TE modes of the parallel-plate waveguide in general, using the mixed basis functions, and along the same line as the standard formulation given by Harrington [1]. After the terms in the waveguide integral equation are identified with the basis functions, the scattering by a cylindrical obstacle (in waveguides, regular sized and oversized, with several propagating modes) is studied. The method is then applied to the scattering by a inhomogeneous waveguide junction with two different dielectrics. For convenience in both studies, the point-matched weighting functions are used.

Only a *small* number of basis functions are needed for the moment method using the mixed basis functions. The reason is the following. One type of the basis functions is used to represent the propagating modes along the infinite waveguide walls; there are only a few of these propagating modes. The other type (say, the narrow unit-pulse functions) is used to represent the evanescent waves; the evanescent waves are highly localized at the obstacle.

The numerical integration of the basis functions of the propagating mode is simplified and quickened by a field transformation. The derivation of the transformation is presented in the Appendix.

Manuscript received August 7, 1972; revised January 8, 1973. This work was supported by the National Research Council of Canada under Operating Grant A3804.

The authors are with the Department of Electrical Engineering, University of Waterloo, Waterloo, Ont., Canada.

II. General Formulation with Mixed Basis Functions

The methods of moment may be used to solve the following inhomogeneous equation

$$\tilde{L}(f) = g \tag{1}$$

where $\tilde{L}$ is a linear operator, g is a known function, and f is to be determined. Instead of expanding f into a standard series of a single type of basis functions, as given by Harrington [1], we shall expand f into a series of the mixed type, say of two types, of basis functions, f_n and h_n. That is,

$$f = \sum_{n=1}^{N_0} \alpha_n f_n + \sum_{n=1}^{N_1} \beta_n h_n \tag{2}$$

where α_n and β_n are the coefficients. The above expansion is allowed as long as f_n and h_n are linearly independent in the domain of $\tilde{L}$. These basis functions, similar to those in a standard series, need not be orthogonal nor complete [3]. Substituting (2) into (1) and using the linearity of $\tilde{L}$, we have

$$\sum_{n=1}^{N_0} \alpha_n \tilde{L}(f_n) + \sum_{n=1}^{N_1} \beta_n \tilde{L}(h_n) = g. \tag{3}$$

It is evident that the suitable inner product $\langle f, g \rangle$ need not be changed by the mixed type of basis functions. Now the weighting functions can be defined either as a mixed- or a single-type series. For convenience in this paper, we may define them as a single type w_m in the range of $\tilde{L}$. Thus, taking the inner product of (3) with each w_m, we get

$$\langle w_m, g \rangle = \sum_{n=1}^{N_0} \alpha_n \langle w_m, \tilde{L} f_n \rangle + \sum_{n=1}^{N_1} \beta_n \langle w_m, \tilde{L} h_n \rangle \tag{4}$$

with $m = 1, 2, 3, \cdots, N_0 + N_1$.

This set of equations can again be written in the standard matrix form as given by Harrington [1]:

$$\{g_m\} = [l_{m,n}] \begin{bmatrix} \{\alpha_n\} \\ \{\beta_n\} \end{bmatrix} \tag{5}$$

where $\{\alpha_n\}$, $\{\beta_n\}$, and $\{g_m\}$ are again, respectively, the unknown and known column matrices. Each square matrix element $l_{m,n}$ is given by the inner product of either $\langle w_m, \tilde{L} f_n \rangle$ or $\langle w_m, \tilde{L} h_n \rangle$. Since the basis-function types, f_n and h_n, are mixed, the matrix-element type is also mixed. In spite of this the square matrix in (5) can obviously still be inverted by a standard method to get the unknown α_n and β_n.

III. The Integral Equation for TE Modes in a Parallel-Plate Waveguide

In a source-free *two-dimensional* space $\boldsymbol{r}(x, z)$, the transverse electric field E_y is given by the *line* integrals of all the electric- and the equivalent magnetic-current densities, $\boldsymbol{J}$ and $\boldsymbol{M}$, along the closed boundary of the space. That is [7],

$$\mathfrak{P} E_y(\boldsymbol{r}) = -j\omega\mu_0 \oint' J\boldsymbol{r}' G(\boldsymbol{r} \mid \boldsymbol{r}')\, d\boldsymbol{r}' - \nabla_t \times \oint' \boldsymbol{M}(\boldsymbol{r}') G(\boldsymbol{r} \mid \boldsymbol{r}')\, d\boldsymbol{r}' \tag{6}$$

where

$$G(\boldsymbol{r} \mid \boldsymbol{r}') = \frac{1}{j4} H_0^{(2)}(\sqrt{\epsilon_r} k \mid \boldsymbol{r} - \boldsymbol{r}' \mid), \qquad k^2 = \omega^2 \mu_0 \epsilon_0 \tag{6a}$$

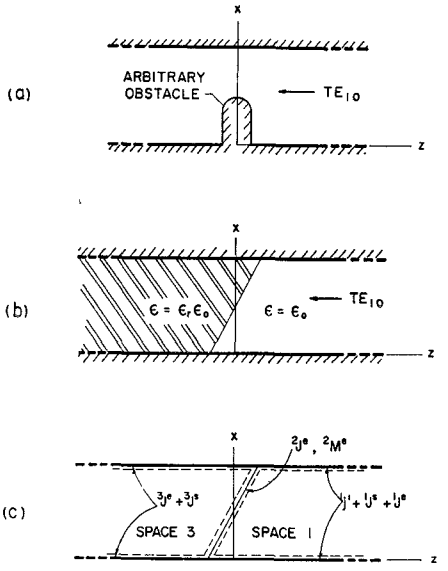

Fig. 1. (a) The homogeneous waveguide junction. (b) The inhomogeneous waveguide junction. (c) The inhomogeneous junction separated into two homogeneous dielectric spaces, with the incident, scattered, and evanescent components of the electric and magnetic currents, as well as the field points, marked on their boundaries. Dotted lines indicate field-point locations.

i.e., the Green's function is the zeroth-order Hankel function of the second kind. The space is assumed to be homogeneously filled with a medium of dielectric constant ϵ_r. The two-dimensional curl $(\nabla_t \times)$ in the second term operates on the field point $\boldsymbol{r}$, while the line integrals in both terms operate on the source point $\boldsymbol{r}'$. The electric- and magnetic-current densities on the waveguide walls are related to the magnetic and electric fields there by the vector relations

$$\begin{aligned} \boldsymbol{J} &= \hat{n} \times \boldsymbol{H} \\ \boldsymbol{M} &= \boldsymbol{E} \times \hat{n} \end{aligned} \tag{7}$$

where $\hat{n}$ is the unit vector normal to the line boundary. As we have assumed $\boldsymbol{E}$ to lie on the y direction and $\boldsymbol{H}$ to lie on the x–z plane, it is clear that $\boldsymbol{J}$ has only the y component, and the components of $\boldsymbol{M}$ lie on the x–z plane.

IV. Homogeneous Junction

The identification of the moment-method matrix with the integral equation given in (6) is rather involved since the equation has two integral operators. For clarity, therefore, in the first identification we shall eliminate the integral operator involving the magnetic current $\boldsymbol{M}$. This is done by considering the homogeneous junctions with only conductive obstacles. In this way, as shown in Fig. 1(a), the line integral for homogeneous space can be made to integrate along the boundaries of the conducting obstacles and the infinite waveguide walls. On these boundaries E_y and, therefore, $\boldsymbol{M}$ are zero.

With the second integral operator eliminated, (6) can be arranged to have a form similar to (1) with the known and unknown parameters on the opposite sides of the equal sign. To do this, we shall first decompose the electric current J_y in (6) into a sum of the incident modal current $j_a{}^i$, the total scattered propagating current J^s and the total scattered evanescent current J^e, i.e.,

$$J_y = j_a{}^i + J^s + J^e. \tag{8}$$

Without loss of generality, the incident modal current $j_a{}^i$ is

assumed to be that of a single TE_{a0} mode[1] with unit amplitude. The subscript y has been dropped in the right-hand side since all currents are assumed to flow in the y direction. For convenience, all currents on the obstacle, propagating and evanescent, are lumped together as an evanescent current. With (8) substituted into (6), and with the E_y and M set to zero on the conducting boundary, we get the rearranged form of (6) as

$$j\omega\mu_0 \oint' j_a{}^i G(r \mid r')\, dr' = -j\omega\mu_0 \oint' (J^s + J^e) G(r \mid r') dr'. \quad (9)$$

The above equation can be identified with (1) since $j_a{}^i$, and therefore its electric-field integral at the left-hand side, is a completely known function; the unknown function at the right-hand side is not the corresponding field integral but the scattered current (J^s+J^e) acted on by the integral operator with the kernel G.

Now we expand the total scattered current into two basis function types. First, the propagating current is written as a basis function sum of the $2N_0$ propagating modes with unit amplitude, i.e.,

$$J^s = \sum_{n=1}^{N_0} [R_n j_n{}^r(r') + T_n j_n{}^t(r')] \quad (10)$$

where R_n and T_n are the reflection and transmission coefficients of the TE_{n0} propagating modes. It is noted that all the reflected modal currents $j_n{}^r$, as well as the incident $j_a{}^i$, are semi-infinite in extent, that is they have value only on the *walls* to the incident side of the waveguide junction. A similar condition, but to the opposite side, is true for all the transmitted modal current $j_n{}^t$. Next the localized evanescent current is written as a basis-function sum of N_1 unit pulses:

$$J^e = \sum_{n=1}^{N_1} \alpha_n h_n(r') \quad (11)$$

where α_n is the electric-current density at the evanescent source point r', and h_n is a pulse function of unit amplitude and a fixed width $\Delta r'$. Although the basis functions $j_n{}^r, j_n{}^t$, and h_n are not orthogonal to each other, they are obviously linearly independent as required by the moment method.

With the width $\Delta r'$ being small, (10) and (11) can be substituted into (9) to reduce the latter into the following sum:

$$-e_a{}^i(r) = \sum_{n=1}^{N_0} [R_n e_n{}^r(r) + T_n e_n{}^t(r)] - j\omega\mu_0 \sum_{n=1}^{N_1} \alpha_n G(r \mid r_n') \Delta r' \quad (12)$$

where the semi-infinite line integral

$$e_n{}^p(r) = -j\omega\mu_0 \int' j_n{}^p(r') G(r \mid r')\, dr', \qquad p = i, r, \text{ or } t \quad (12a)$$

[1] The second index of the mode is always zero, since there is no field variation in the y direction for a parallel-plate waveguide defined on the x-z plane as in Fig. 1(a).

is the partial electric field due to the known semi-infinite wall current of the TE_{n0} propagating mode. The numerical evaluation of $e_n{}^p$ can be performed either through a transformation given by Wu and Chow [6], or more conveniently through another transformation given in the Appendix.

Having the same form as (3), (12) can now be solved by forming the standard matrix of the moment method. The weighting functions are chosen to be a series of Dirac δ-functions, i.e.,

$$w_m = \delta(r - r_m), \qquad m = 1, 2, \cdots, 2N_0 + N_1 \quad (13)$$

where the field points r_m are matched such that N_1 of them are the evanescent source points of the basis functions while the other $2N_0$ points, matching to the propagating modes, are arbitrarily selected points on the waveguide walls beyond the evanescent region. Taking the inner product of (12) with each w_m in (13) we get the sum

$$-e_a{}^i(r_m) = \sum_{n=1}^{N_0} [R_n e_n{}^r(r_m) + T_n e_n{}^t(r_m)] - j\omega\mu_0 \sum_{n=1}^{N_1} \alpha_n G(r_m \mid r_n') \Delta r'. \quad (14)$$

Equation (14) is identified with (4). Hence a standard matrix of the type in (5) can be formed.

Before the matrix can be inverted it is noted that in the second sum, the function G, as given in (6a), diverges when the field point r_m coincides with the source point r_n'. For these points, we have to replace G by a more suitable approximation:

$$G(r_m \mid r_n') = \frac{1}{j4}\left[1 - j\frac{2}{\pi}\left(\ln\frac{k\Delta r'}{4} + \gamma - 1\right)\right], \qquad r_m = r_n' \quad (14a)$$

where $\gamma = 0.577215$, as given by Harrington [1].

With the matrix inverted, the unknown coefficients R_n, T_n, and α_n of the currents are obtained.

V. Inhomogeneous Junction

For an inhomogeneously filled waveguide junction, as shown in Fig. 1(b), the homogeneous space equation (6) cannot be applied directly. It is necessary, hence, to consider the junction as two separated but homogeneous and closed dielectric spaces. These two spaces have a dielectric interface; therefore, the magnetic-current term in (6) has to be included to account for the contribution from the equivalent magnetic current ($M = E \times \hat{n}$) across the interface.

The magnetic-current term in (6) is not in a form suitable for numerical analysis. To improve this we shall first move the field-point differential operator $\Delta_t \times$ through the source-point integral operator into the integrand. Then the integrand is transformed into two terms, which are

$$\nabla_t \times [M(r')G(r \mid r')] = G(r \mid r')\nabla_t \times M(r') - M(r') \times \nabla_t G(r \mid r') \quad (15)$$

from a standard vector relation. The first term in the above vanishes since the field-point operator $\Delta_t \times$ does not operate on the source points in M; and the second term above, involving the gradient ∇_t, can be easily differentiated since its operand, the Green's function, is simply a zeroth-order Hankel function. With the integrand of the second term in (6) thus re-

duced, it can be substituted back into (6) to get the more convenient form:

$$E_y(r) = -j\omega\mu_0 \oint' J_y G(r \mid r')\, dr' + \hat{y} \cdot \oint' M^e \times G'(r \mid r')\, dr' \quad (16)$$

where the vector

$$G'(r \mid r') = \nabla_i G(r \mid r') = \frac{-\sqrt{\epsilon_r}k}{j4} \frac{(r - r')}{|r - r'|} H_1^{(2)}(\sqrt{\epsilon_r}k \mid r - r' \mid) \quad (16a)$$

with ϵ_r being the dielectric constant of a separated space of the inhomogeneous junction.

The boundary condition requires that the tangential E- and H-fields are continuous across the interface between the two separated spaces. Nevertheless, their equivalent electric and magnetic currents as given in (7) have opposite signs in the two separated spaces since the unit vector $\hat{n}$ changes sign across the interface.

With these in mind, we may now decompose the currents J and M of (6) into the following superscripted current-density components. Along the waveguide walls at the incident side of the dielectric interface:

$^1j_a{}^i$ modal current of incident TE_{a0} mode of unit amplitude;

$^1J^s$ current of all scattered propagating modes;

$^1J^e$ current of all evanescent modes. (17)

Along the waveguide walls at the transmission side there is no incident current, while there are both the scattered propagating and evanescent currents $^3J^s$ and $^3J^e$. In between these two spaces, along the interface itself, and with the upper sign referring to the incident side, we define

$\pm{}^2J^e$ *total* scattered electric current;

$\pm{}^2M^e$ *total* scattered magnetic current. (17a)

For easy identification in the following integrals and matrix, the superscripted currents and the corresponding sections are drawn in Fig. 1(c). Outside their defined sections, the currents are assumed to be zero.

With the relevant currents substituted and in the space at the incident side, (6) can be written in a form similar to (9), but with line integrals only along the boundaries with the specific currents,

$$j\omega\mu_0 \int_1' {}^1j_a{}^{i1}G(r \mid r')\, dr' = -j\omega\mu_0 \left[\int_1' ({}^1J^s + {}^1J^e) + \int_2' {}^2J^e \right] {}^1G(r \mid r')\, dr' + \hat{y} \cdot \int_2' {}^2M^e \times {}^1G'(r \mid r')\, dr' - {}^2M^e(r) \quad (18)$$

where, similar to the subscripted integrals, the Green's functions are superscripted to indicate the dielectric space they belong to. It is noted that the E_y-field along the interface is replaced by its equivalent magnetic current $^2M^e$. Similarly, in the space at the transmission side, (6), with the incident current equal to zero is

$$0 = -{}^2M^e(r) - \hat{y} \cdot \int_2' {}^2M^e \times {}^3G'(r \mid r')\, dr' + j\omega\mu_0 \left[\int_2' {}^2J^e - \int_3' ({}^3J^e + {}^3J^s) \right] {}^3G(r \mid r')\, dr'. \quad (19)$$

Similar to the expansion in (10) and (11), we can now expand the currents $^1J^s$, $^1J^e$, $^2J^e$, $^2M^e$, $^3J^e$, and $^3J^s$ into two types of basis functions, of propagating modes, and of unit pulses. Therefore, equivalent to (12), (18) and (19) can be written into the two following sums: with the field and source points defined as r_m and r_n', at the incident side the sum is[2]

$$-{}^1e_a{}^i(r_m) = \sum_{n=1}^{N_0} R_n {}^1e_n{}^r(r_m) - j\omega\mu_0 \sum_{n=1}^{N_1} {}^1\alpha_n {}^1G(r_m \mid r_n')\, \Delta r' - j\omega\mu_0 \sum_{n=1}^{N_2} {}^2\alpha_n {}^1G(r_m \mid r_n')\, \Delta r' - \sum_{n=1}^{N_2} {}^2\beta_n {}^1F(r_m \mid r_n')\, \Delta r' \quad (20)$$

at the transmission side the sum is

$$0 = j\omega\mu_0 \sum_{n=1}^{N_2} {}^2\alpha_n {}^3G(r_m \mid r_n')\Delta r' - \sum_{n=1}^{N_2} {}^2\beta_n {}^3F(r_m \mid r_n')\, \Delta r' - j\omega\mu_0 \sum_{n=1}^{N_3} {}^3\alpha_n {}^3G(r_m \mid r_n')\, \Delta r' + \sum_{n=1}^{N_4} T_n {}^3e_n{}^t(r_m) \quad (21)$$

where $^2\beta_n$ is the *magnetic*-current density at the evanescent source point r_n' on the interface. The Green's function for magnetic current is

$$^{1,3}F(r_m \mid r_n') = \hat{y} \cdot \left(\frac{M}{|M|} \right) \times {}^{1,3}G'(r_m \mid r_n'), \qquad r_m \neq r_n' \quad (22)$$

$$= 1/2\Delta r', \qquad r_m = r_n'. \quad (22a)$$

For $r_m = r_n'$, the first F term in (22) diverges and, as shown by Harrington [1], the second F term in (22a) has to be used. It is noted that the $^2M^e(r)$ terms in (18) and (19) have been absorbed in the second F term.

The field-point testing functions w_m are again a sequence of Dirac δ-functions coinciding with the centers of the unit pulses of the evanescent waves. At each unit pulse along the interface there are actually two source-current quantities, one electric and one magnetic. Therefore, corresponding to each source point, two field-point testing functions are needed, one slightly to the right in space 1 and the other slightly to the left in space 3. With all the evanescent field points and source points matched, a few arbitrary field points, on the waveguide walls at each side of the interface beyond the evanescent region, are needed to match the scattered propagating modes. In this way, the number of equations arrived at from the field point equals the number of unknown mode and pulse basis functions, and the matrix for the moment method is formed. Thus, following (20) and (21), the matrix has a size of $N \times N$ where $N = N_0 + N_1 + 2N_2 + N_3 + N_4$. For clarity, the matrix is partitioned in the following submatrices:

[2] The partial electric fields $^{1,3}e_n{}^p$ here are the same semi-infinite line integrals of the modal current as those in (12a). Nevertheless, an extra superscript is added at the upper left-hand corner to indicate the dielectric space, 1 or 3 in Fig. 1(c), in which they have nonzero values. The corresponding modal current, such as $^1j_a{}^i$ in (17) had the same superscripts.

$$\begin{bmatrix} -\{{}^1e_a{}^i\} \\ -\{{}^1e_a{}^i\} \\ -\{{}^1e_a{}^i\} \\ \{0\} \\ \{0\} \\ \{0\} \end{bmatrix} = \begin{bmatrix} [{}^1e_n{}^r] & [{}^1G] & [{}^1G] & [{}^1F] & [0] & [0] \\ [{}^1e_n{}^r] & [{}^1G] & [{}^1G] & [{}^1F] & [0] & [0] \\ [{}^1e_n{}^r] & [{}^1G] & [{}^1G] & [{}^1F] & [0] & [0] \\ [0] & [0] & [{}^3G] & [{}^3F] & [{}^3G] & [{}^3e_n{}^t] \\ [0] & [0] & [{}^3G] & [{}^3F] & [{}^3G] & [{}^3e_n{}^t] \\ [0] & [0] & [{}^3G] & [{}^3F] & [{}^3G] & [{}^3e_n{}^t] \end{bmatrix} \cdot \begin{bmatrix} & \{R_n\} & \\ -j\omega\mu_0 & \Delta r' & \{{}^1\alpha_n\} \\ -j\omega\mu_0 & \Delta r' & \{{}^2\alpha_n\} \\ -\Delta r' & \{{}^2\beta_n\} & \\ -j\omega\mu_0 & \Delta r' & \{{}^3\alpha_n\} \\ & \{T_n\} & \end{bmatrix} \cdot \quad (23)$$

The column matrices $\{{}^2\alpha_n\}$ and $\{{}^2\beta_n\}$ represent the $2N_2$ pulse-function coefficients of the electric and magnetic source currents on the dielectric interface. The third column matrix $-\{{}^1e_a{}^i\}$ and the following null matrix $\{0\}(=\{{}^3e_a{}^i\})$ are the partial electric field due to the incident mode current $j_a{}^i$ *on the same interface* but slightly to the incident and the transmission sides, i.e., in spaces 1 and 3. Since the column matrices for the field points at the interface are for points different, though very slightly, from the source points, it is well understood that the square matrix above is not diagonally symmetrical in its arrangement of null submatrices.

The last three field column matrices in (23) are null matrices since we have assumed no incident wave field at the transmission side, as observed in the integral equation of (21).

Now, the first three field column matrices $\{{}^1e_a{}^i\}$ at the left-hand side and all the submatrices $[{}^{1,3}e_n{}^{r,t}]$ at the right-hand side can be calculated from the Appendix. Together with $[{}^{1,3}G]$ and $[{}^{1,3}F]$ calculated from (6a), (14a), (22), and (22a), the matrix in (23) can be inverted to get all the unknown reflection, transmission, and evanescent-current coefficients R_n, T_n, α_n, and β_n.

Simplification in the inversion of (23) is possible on account of its partial symmetry and null matrices. In particular in this paper, matrix simplifications following Preis [9] and Pipes [10] are used. These are standard simplifications, but the applications of them vary with the matrices formed by different boundary conditions. Therefore, the details of the simplifications are not included.

VI. Numerical Examples

All the reflection and transmission coefficients derived were those of the wall current J_y. However, the usual definition of these coefficients are those of the electric field, i.e., E_y in our case; therefore, for easy comparison of the numerical examples with the available solutions, a conversion is needed. By comparing the fields E_y and H_z (and hence J_y) of the TE_{n0} mode in a parallel-plate waveguide [8], the following conversion is obtained.

$$R_n\big|_{\text{for } E_y} = \left(\frac{a}{n}\right) R_n\big|_{\text{for } J_y}$$

$$T_n\big|_{\text{for } E_y} = \left(\frac{a}{n}\right) T_n\big|_{\text{for } J_y}. \quad (24)$$

A TE_{a0}-mode incidence is assumed.

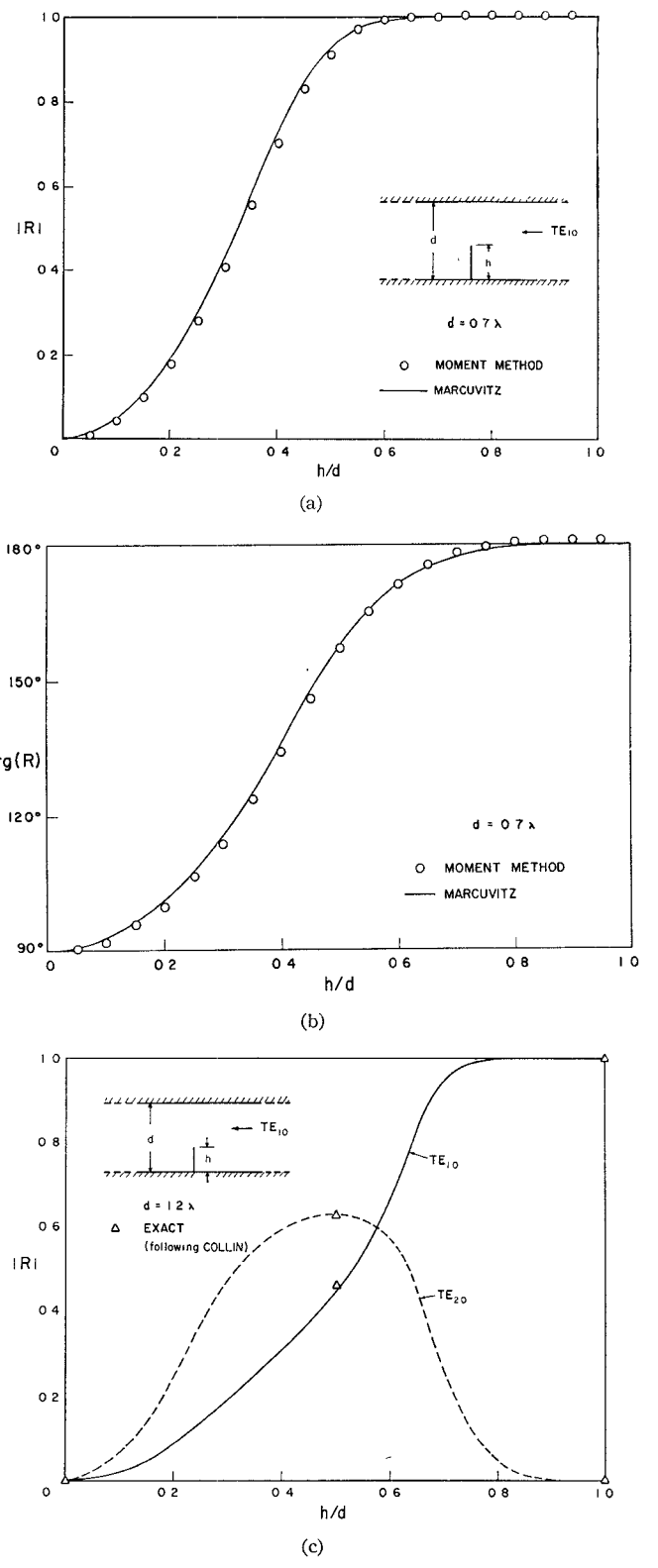

Fig. 2. Parameters of the reflection coefficients, from the homogeneous junction as a function of diaphragm height. TE_{10}-mode incidence is assumed. (a) TE_{10} magnitudes. (b) Phases for width $d=0.7\ \lambda$. (c) Magnitudes only for the oversized width $d=1.2\ \lambda$.

Homogeneous Junction

The moment method is first applied to a waveguide with a thin conducting diaphragm in Fig. 2. The incident mode is assumed to be TE_{10} of unit amplitude. Calculated from the matrix formed by the linear equation (14) and converted by

(24), the E_y reflection coefficients are plotted as functions of the diaphragm height h for waveguide widths of 0.7λ and 1.2λ.

The solutions for $d=0.7\lambda$ by Marcuvitz [8, pp. 224–227] is included for comparison; good agreement between the two sets of solutions is observed. In the case of $d=1.2\lambda$, exact solutions are available only for three values of h: for $h=0$ and $h=d$, the solutions are trivial; and for $h=d/2$, exact solutions are obtained following Collin's procedure [11]. For these three h/d ratios, the agreement of solutions is good. Therefore, it is reasonable to assume that the moment-method solutions for other h/d ratios are dependable.

Inhomogeneous Junctions

No solutions, exact or approximate, for the slanting dielectric interface in Fig. 1(b), are available. To test the method, therefore, the exact solution [12] and moment-method solution, calculated from the matrix in (23) with the conversion in (24) of a junction with perpendicular interface, were computed and compared. No discrepancy between the solutions was detected.

Having tested the method, we consider the junctions with slant interface. The computed E_y reflection and transmission coefficients are plotted in Figs. 3 and 4 for waveguide widths of 0.7λ and 1.2λ, and for slant ratios L/d of 2/7 and 1. As a check for the accuracy of the solutions, we sum the total scattered powers which should add to 100 percent of the incident powers. The sums are included in Figs. 3 and 4. It is observed that their errors are within 5 percent for frequencies not too close to the cutoffs.

VII. Discussion

In each application of the moment method stated above, the scattered propagating currents are expanded in terms of only a few modal basis functions. Hence, the convergence of the method depends upon the extent of the evanescent current region which decides the number of pulse basis functions used. For electrically small junctions, the convergence is rapid.

In view of the complexity of (18) and (19) of the inhomogeneous junctions as compared to (9) of the homogeneous junctions, it is expected that the number of the pulse basis functions needed for the former is much greater than that for the latter. For the homogeneous and inhomogeneous junctions in Figs. 2(a), (c), 3(b), 4, and 3(c), these numbers are 16, 20, 39, 49, and 57, respectively. The relative computing times are: 1, 1.5, 8, 12, and 17. As the junction becomes larger and larger, more and more basis functions are required to cover the widely extended evanescent current. This spoils the convergence of the problem. Therefore, especially for the inhomogeneous cases, the method is useful only for junctions not too large electrically.

A technique for the numerical computation of the integral of a propagating mode current in (12a) has been suggested by Wu and Chow [6]. In the Appendix, a better approach through a field transformation has been given. This approach results in a numerical computation both with better accuracy and reduced (to about half) computing time.

Only TE_{n0} modes of the parallel-plate waveguide are studied in this paper. One reason is that their fundamental TE_{10} modes are identical to the important fundamental modes in the familiar rectangular waveguide. The other rea-

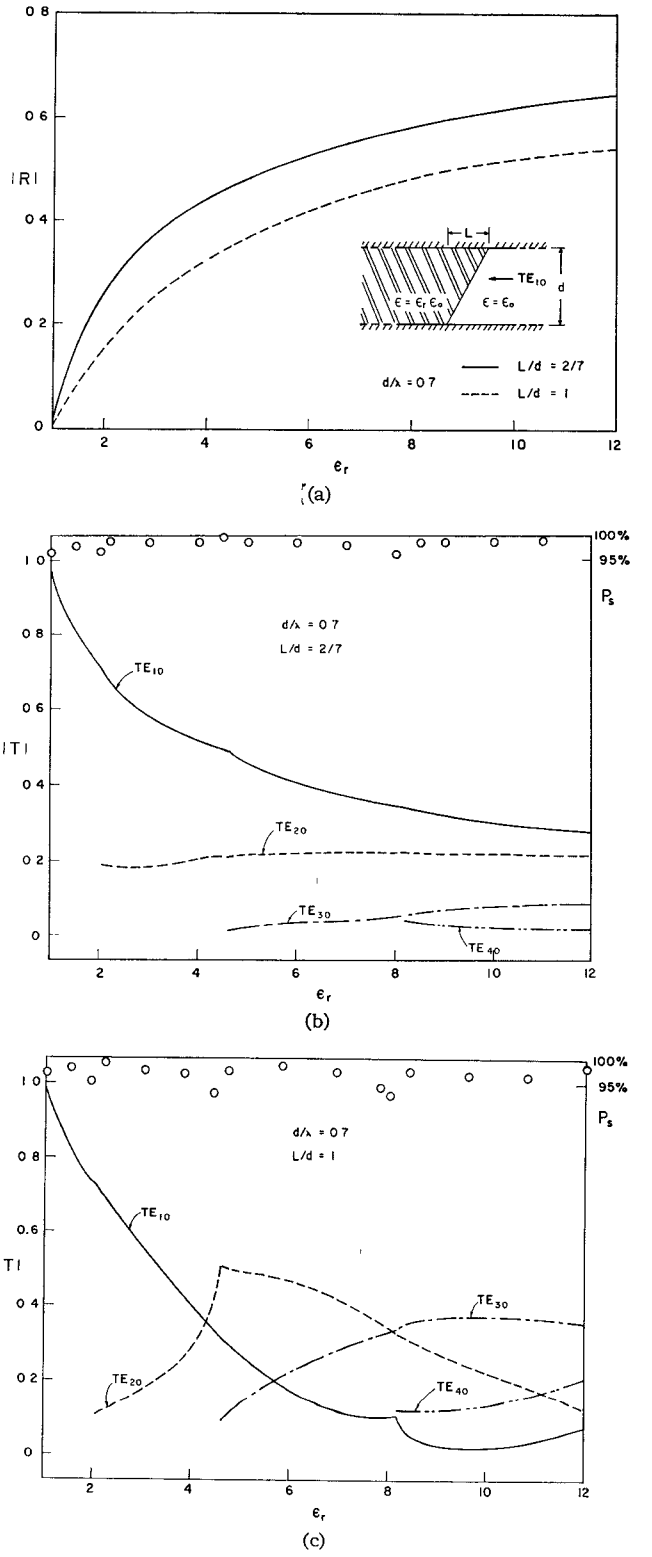

Fig. 3. The magnitudes of reflection coefficients and the sum of powers of the propagating modes from the inhomogeneous junction, as a function of the dielectric constant. TE_{10}-mode incidence with $d=0.7\lambda$ are assumed. (a) The only reflected mode with junction slant ratios $L/d=2/7$ and 1. (b) The four transmitted modes with $L/d=2/7$. (c) The four transmitted modes with $L/d=1$.

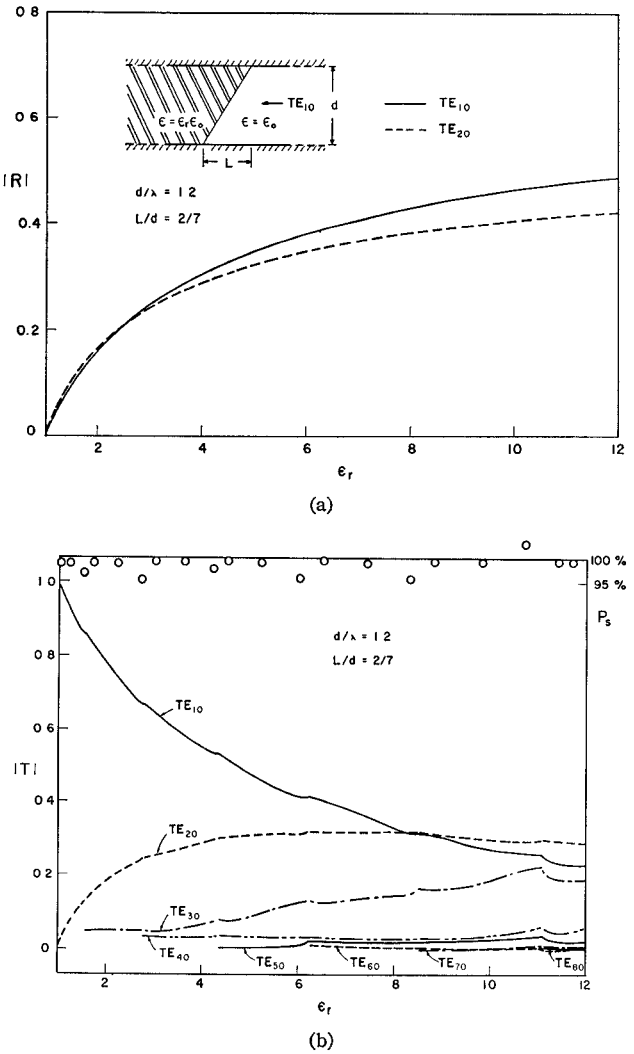

Fig. 4. Similar graph parameters as in Fig. 3, except that the waveguide is oversized even in the incident side, i.e., $d = 1.2\lambda$. (a) Two reflected modes with $L/d = 2/7$. (b) Eight transmitted modes with $L/d = 2/7$.

son is that to illustrate the use of the mixed basis functions, it may be clearer to study modes with simple boundary conditions; the TE boundary conditions used in (9), (18), and (19) of the parallel-plate waveguide satisfied this condition.

At the end it is pointed out that Mautz and Harrington [13] were the first investigators to use the mixed basis functions consisting of modal functions for the azimuthal variation and pulse functions for the polar variation. This paper, however, is the first to use the mixed basis functions, modal and pulse, simultaneously along the same coordinate variation, i.e., along the same waveguide walls.

Appendix

A transformation needed to numerically evaluate the *semi-infinite* line integral to get the electric field from the wall current of a *single propagating mode* along a semi-infinite parallel-plate waveguide in a homogeneous dielectric space is derived as follows. Let the propagating mode be the incident TE_{n0} with a known wall current j_n^i. The *unknown* electric field to be integrated from the modal current according to (12b) is

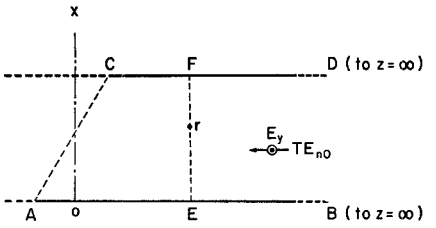

Fig. 5. The transformed paths of integration for the semi-infinite line integral in the Appendix.

$$e_n^i(\mathbf{r}) = -j\omega\mu_0 \int'_{AB+CD} j_n^i(\mathbf{r}')G(\mathbf{r}\,|\,\mathbf{r}')\,d\mathbf{r}'. \quad \text{(A-1)}$$

The paths of integration along AB and CD on the walls of the semi-infinite waveguide are as shown in Fig. 5. For generality the edges A and C of the walls are drawn staggered. The field point $\mathbf{r}$ can be anywhere. In Fig. 5, however, it is drawn inside the waveguide.

Let a short-circuit wall be placed along the line EF perpendicular to the walls and passing through the field point $\mathbf{r}$. The zero electric field resulting is actually the line integral of the known incident and reflected modal current j_n^i and j_n^r on *the short-circuit* wall EF and on the waveguide walls EB and FD. As shown in Fig. 5 walls $EB = AB - AE$, $FD = CD - CF$. Therefore, the zero electric field at the short-circuit wall can be written as

$$0 = -j\omega\mu_0\left[\int'_{AB+CD} - \int'_{AE+CF} + \int'_{EF}\right] \cdot [j_n^i + j_n^r]G(\mathbf{r}\,|\,\mathbf{r}')\,d\mathbf{r}'. \quad \text{(A-2)}$$

Next let an open-circuit wall be placed along the same line EF. The electric field resulting is twice the *known* electric field $\mathcal{E}_n^i(\mathbf{r})$ of the incident mode. Therefore, the electric field at the open circuit can be written as

$$2\mathcal{E}_n^i(\mathbf{r})\,|_{\mathbf{r}\text{ on }EF} = -j\omega\mu_0\left[\int'_{AB+CD} - \int'_{AE+CF}\right][j_n^i - j_n^r]G(\mathbf{r}\,|\,\mathbf{r}')\,d\mathbf{r}' + \hat{y}\cdot\int'_{EF} 2\mathbf{m}_n^i \times \mathbf{G}'(\mathbf{r}\,|\,\mathbf{r}')\,d\mathbf{r}'. \quad \text{(A-3)}$$

On comparing (A-2) to the above it is noted that the reflected current j_n^r changes sign from short circuit to open circuit. Also the last integral along EF is integrated not over the electric current but over the magnetic current, since the electric current is zero at the open circuit. The Green's function $\mathbf{G}'$ for the magnetic current is defined in (16a) in Section V.

Along the open circuit EF, like the electric field, the magnetic current is twice the incident value, i.e., $2\mathbf{m}_n^i$. This is because the magnetic current is related directly to the electric field at the same point by the vector relation $2\mathbf{m}_n^i = 2\mathcal{E}_n^i \times \hat{n}$, where $\hat{n}$ is the unit normal of the wall EF. Conversely, then, as pointed out by Harrington [1], the electric field resulting

from the integration of the $2\boldsymbol{m}_n{}^i$ in the last integral in (A-3) must equal one-half of the electric field ($2\mathcal{E}_n{}^i$), i.e., having a magnitude $\mathcal{E}_n{}^i$. With this magnitude substituted, (A-3) is reduced to

$$\mathcal{E}_n{}^i(\boldsymbol{r})\,|_{\boldsymbol{r}\text{ on }EF} = -j\omega\mu_0\left[\int'_{AB+CD} - \int'_{AE+CF}\right] \cdot [j_n{}^i - j_n{}^r]G(\boldsymbol{r}\,|\,\boldsymbol{r}')\,d\boldsymbol{r}'. \quad \text{(A-4)}$$

On summing (A-2) and (A-4), all integrals involving the reflected current $j_n{}^r$ are cancelled except for that along the short-circuit wall EF. Along this short-circuit wall $j_n{}^r$ is identical and replaceable by $j_n{}^i$. Hence, the rearranged result of the summation can be written completely in terms of the incident terms, which is

$$-j\omega\mu_0\int'_{AB+CD} j_n{}^i(\boldsymbol{r}')G(\boldsymbol{r}\,|\,\boldsymbol{r}')\,d\boldsymbol{r}' = \frac{1}{2}\mathcal{E}_n{}^i(\boldsymbol{r})\,|_{\boldsymbol{r}\text{ on }EF} + j\omega\mu_0\left[\int'_{EF} - \int'_{AE+CF}\right] j_n{}^i(\boldsymbol{r}')G(\boldsymbol{r}\,|\,\boldsymbol{r}')\,d\boldsymbol{r}'. \quad \text{(A-5)}$$

All terms at the right-hand side are known; these include the electric field $\mathcal{E}_n{}^i$ of the incident mode and the partial electric fields integrated from the known current $j_n{}^i$ of the same mode. The paths of integration EF, AE, and CF are short, and therefore can easily be numerically integrated.

The electric-field integral at the left-hand side is the unknown $e_n{}^i(\boldsymbol{r})$ we need in (A-1). Thus the semi-infinite line integral of (A-1) is transformed into short, numerically evaluable, line integrals in (A-5).

The field point $\boldsymbol{r}$ in (A-5) can be anywhere, including that beyond the waveguide edges AC in Fig. 5. In this case, the walls AE and CF become extensions from the waveguide edges, and the last integral in (A-5) should be added to instead of subtracted from the right-hand side.

It is observed that the above derivation for the transformation can be applied equally well for the reflected current $j_n{}^r$. The only difference is that instead of summing (A-4) to (A-2), (A-4) is subtracted from (A-2). The resulting transform equation (A-5) for $j_n{}^r$ is identical to that for $j_n{}^i$, except for the $-(1/2)\mathcal{E}_n{}^i(\boldsymbol{r})$ instead of a positive one at the right-hand side.

Also it is observed that the transform equation (A-5) for the reflected current $j_n{}^r$ can be applied directly for the transmitted current $j_n{}^t$, since they are both propagating away from the edge AC in Fig. 5.

The transform equations for $j_n{}^i$, $j_n{}^r$, and $j_r{}^t$ are applied to calculate the partial electric fields $e_a{}^i$, $e_n{}^r$, and $e_n{}^t$ in (12), (20), and (21). It is noted that the partial electric fields in the two latter equations are superscripted at the left-hand corner to indicate the dielectric space, 1 or 3 in Fig. 1(c), in which they are to be calculated.

References

[1] R. F. Harrington, *Field Computation by Moment Methods*. New York: Macmillan, 1968, pp. 2–61.

[2] N. Morita, "Diffraction by arbitrary cross-sectional semi-infinite conductor," *IEEE Trans. Antennas Propagat.*, vol. AP-19, pp. 358–364, May 1971.

[3] D. S. Jones, *The Theory of Electromagnetism*. New York: Pergamon, 1964, pp. 269–271.

[4] A. Wexler, "Solution of waveguide discontinuities by modal analysis," *IEEE Trans. Microwave Theory Tech.*, vol. MTT-15, pp. 508–517, Sept. 1967.

[5] R. Mittra, T. Itoh, and T. S. Li, "Analytical and numerical studies of the relative convergence phenomenon arising in the solution of an integral equation by the moment method," *IEEE Trans. Microwave Theory Tech.*, vol. MTT-20, pp. 96–104, Feb. 1972.

[6] S. C. Wu and Y. L. Chow, "An application of the moment method to waveguide scattering problems," *IEEE Trans. Microwave Theory Tech.*, vol. MTT-20, pp. 744–749, Nov. 1972.

[7] R. F. Harrington, *Time-Harmonic Electromagnetic Fields*. New York: McGraw-Hill, 1961, pp. 120–132 and 223–230.

[8] N. Marcuvitz, *Waveguide Handbook*. New York: McGraw-Hill, 1951, p. 65.

[9] D. H. Preis, "The Teoplitz matrix: Its occurence in antenna problems and a rapid inversion algorithm," *IEEE Trans. Antennas Propagat.* (Commun.), vol. AP-20, pp. 204–206, Mar. 1972.

[10] L. A. Pipes, *Applied Mathematics for Engineers and Physicists*. New York: McGraw-Hill, 1958, pp. 95–96.

[11] R. E. Collin, *Field Theory of Guided Waves*. New York: McGraw-Hill, 1960, pp. 441–447.

[12] C. G. Montgomery, R. H. Dicke, and E. M. Purcell, *Principles of Microwave Circuits*. New York: McGraw-Hill, 1948, pp. 369–371.

[13] J. R. Mautz and R. F. Harrington, "Generalized network parameters for bodies of revolution," AFCRL Rep. AFCRL-68-0282, May 1968.